

ticles ($\text{Fe}_3\text{O}_4@Au\text{-cit}$) were prepared by the simple citrate reduction of Au^{3+} . Afterwards, $\text{Fe}_3\text{O}_4@Au\text{-L}$ was synthesized by a fast ligand place-exchange reaction between the citrate and ligand molecules on the $\text{Fe}_3\text{O}_4@Au$ nanoparticles. Then, these $\text{Fe}_3\text{O}_4@Au\text{-L}$ nanoparticles were fully characterized by visible absorption spectroscopy, magnetic susceptibility measurements and transmission electron microscopy (TEM). The $\text{Fe}_3\text{O}_4@Au\text{-L}$ nanoparticles showed good paramagnetic properties, they are well-dispersed in water and stable.

As compared with the synthesis of magnetic nanoparticles,^{25–27} the proposed method is a simple three-step reaction to synthesize water-soluble new ligand-protected Au-coated iron oxide nanoparticles. The advantages of this method are simplicity, short reaction time, low reaction temperature and high reproducibility of results. Furthermore, another important characteristic of our as-prepared L-Au- Fe_3O_4 nanoparticles is that they are well dispersed in water and alcohols. An important aspect of our synthesis of the $\text{Fe}_3\text{O}_4@Au$ nanoparticles is the formation of a gold shell at the iron oxide nanocrystal cores with high monodispersity and controllable surface capping properties, which facilitates the subsequent control and manipulation of the interparticle interactions and reactivities. The introduction of thiol molecules on the surface of the $\text{Fe}_3\text{O}_4@Au$ nanoparticles does not induce the extensive assembly of nanoparticles, as reported by Wang.²⁰

The size of magnetic nanoparticles was characterized by TEM (LEO 912 AB OMEGA). The samples for TEM analysis were prepared as follows: a drop of magnetic nanoparticles was dispersed in Nanopure water. The resulting solution was sonicated for 5 min to obtain better particle dispersion characteristics. A drop of the dispersed solution was then deposited onto a substrate and dried for 20 min at room temperature. The TEM images of $\text{Fe}_3\text{O}_4@Au\text{-L}$ nanoparticles are presented in Figure 1(a) and the bar diagram in Figure 1(b) shows the size distribution and the average particle sizes (30 nm). $\text{Fe}_3\text{O}_4@Au\text{-L}$ nanoparticles are spherical, and the size changes from 20 to 40 nm. Figure 1(c) depicts the electron diffraction pattern of the $\text{Fe}_3\text{O}_4@Au\text{-L}$ nanoparticles, which is consistent with published data²³ on the core-shell structure of the $\text{Fe}_3\text{O}_4@Au\text{-L}$ nanoparticles.

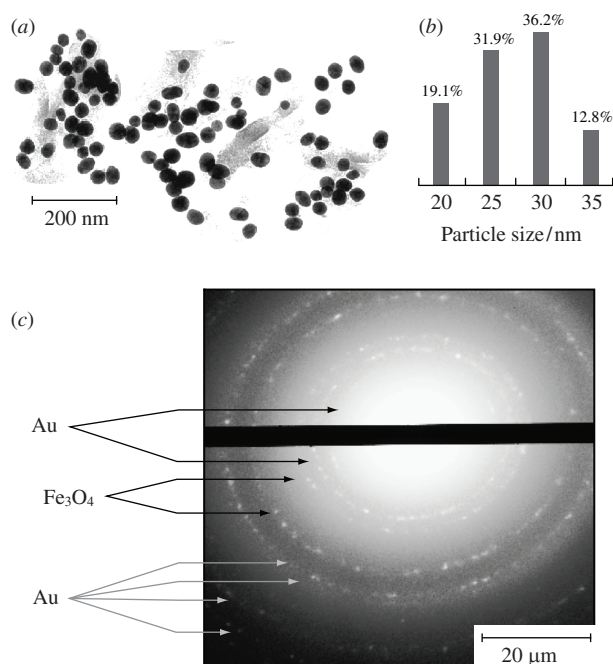


Figure 1 (a) TEM images, (b) size distributions and (c) electron diffraction pattern of $\text{Fe}_3\text{O}_4@Au\text{-L}$ nanoparticles.

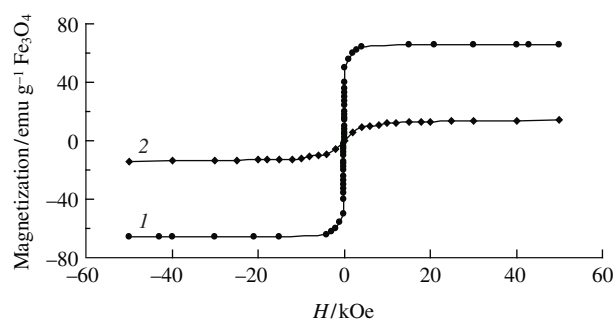


Figure 2 Magnetization hysteresis at 273 K for (1) Fe_3O_4 and (2) $\text{Fe}_3\text{O}_4@Au$ nanoparticles.

Magnetic measurements were performed using a Faraday balance magnetometer. The samples of $\text{Fe}_3\text{O}_4@Au\text{-L}$ nanoparticles were isolated from the aqueous solution by centrifugation and dried in a vacuum.

It has been reported²⁰ that overlaying iron oxide nanoparticle surfaces with a gold shell has a negligible effect on the magnetic behaviour. All the nanoparticles are concentrated at the bottom and right-hand side of the bottle when the magnet is placed at the corresponding positions. Our results demonstrate that the $\text{Fe}_3\text{O}_4@Au\text{-L}$ nanoparticle solution is paramagnetic and the Au atoms are successfully coated on the Fe_3O_4 nanoparticles since a blue colour and paramagnetic properties originate from the gold nanostructure and Fe_3O_4 nanoparticle, respectively. On the other hand, the magnet only attracts the $\text{Fe}_3\text{O}_4@Au\text{-L}$ nanoparticles to the corresponding positions, but it does not promote any precipitation effect. When the permanent magnet is removed, the L-Au- Fe_3O_4 nanoparticles can be re-dispersed in water again. This important characteristic allows the tracking of such particles in a magnetic gradient without losing the advantage of a stable colloidal suspension.

The magnetic properties of the core-shell $\text{Fe}_3\text{O}_4@Au$ nanoparticles were examined and compared with the magnetic properties of Fe_3O_4 .²⁰ The saturation magnetization and blocking temperature were determined from magnetometer Faraday balance measurements. Figure 2 represents the magnetization *versus* magnetic field at 273 K by cycling the field from -50 to 50 kOe. The magnetic data display major differences between Fe_3O_4 and $\text{Fe}_3\text{O}_4@Au$ nanoparticles. First, the magnetization of $\text{Fe}_3\text{O}_4@Au$ is smaller than that of Fe_3O_4 . The maximum magnetization values are 66 and 10 $\text{emu g}^{-1} \text{Fe}_3\text{O}_4$ for Fe_3O_4 and $\text{Fe}_3\text{O}_4@Au$, respectively. The mass of Fe_3O_4 was determined from the loading of magnetic particles in the plastic capsules (0.001 g in this case). Second, the saturation magnetization of $\text{Fe}_3\text{O}_4@Au$ is higher than that of Fe_3O_4 .

To demonstrate the formation of a gold layer around the magnetic nanoparticles, colloidal gold and $\text{Fe}_3\text{O}_4@Au$ solutions were prepared by dissolving Au nanoparticles and $\text{Fe}_3\text{O}_4@Au$, respectively, in 4 ml of water and the absorbance was measured. The visible absorption spectra of the solutions were acquired with a Hitachi U-2900 UV/visible spectrophotometer over the wavelength range of $400\text{--}800$ nm. Figure 3 displays a typical set of the spectra of Fe_3O_4 (curve 1) and $\text{Fe}_3\text{O}_4@Au$ (curves 2 and 3) nanoparticles dispersed in aqueous solution. In contrast to the largely silent feature in the visible region for Fe_3O_4 particles, $\text{Fe}_3\text{O}_4@Au$ particles exhibit bands at 525 and 540 nm for the ligands (citrate and L).

In conclusion, we have proposed a simple three-step reaction to synthesize a new type of ligand-protected water-soluble terpyridine-type $\text{Fe}_3\text{O}_4@Au\text{-L}$ nanoparticles. The attachment of gold atoms by the citrate reduction of Au^{3+} in aqueous solutions finally results in the formation of a very thin gold layer on the surface of the Fe_3O_4 magnetic nanoparticles. This report demon-

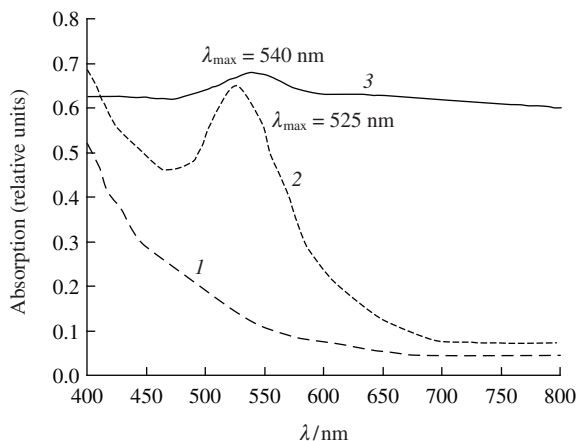


Figure 3 UV-VIS spectra of (1) Fe_3O_4 , (2) $\text{Fe}_3\text{O}_4@Au$ and (3) $\text{Fe}_3\text{O}_4@Au-L$.

strates the place-exchange reaction on gold-coated iron oxide nanoparticles in aqueous solution without the assembly of nanoparticles. The paramagnetic properties, blue colour and TEM data confirm that the Fe_3O_4 nanoparticles are successfully coated with a thin layer of Au atoms. Finally, the TEM data determine the composition and size of the $\text{Fe}_3\text{O}_4@Au-L$ nanoparticles. The attached gold shell provides chemically active sites on the surface of the magnetic nanoparticles, enabling their potential derivatisation with multifunctional organic molecules. In addition, the ligand on the surface of the nanoparticles allows further surface modifications of water-soluble gold-coated magnetic nanoparticles to be carried out for wider applications. Moreover, the characteristics (small particle size, thin layer of Au, good dispersion in water and paramagnetic properties) of the $\text{Fe}_3\text{O}_4@Au-L$ nanoparticles facilitate their catalytic, analytical and biomedical applications.

References

- 1 A. N. Shipway, E. Katz and I. Willner, *Chemphyschem*, 2000, **1**, 18.
- 2 R. W. Wagner, J. S. Lindsey, J. Seth and D. F. Bocian, *J. Am. Chem. Soc.*, 1996, **118**, 3996.
- 3 L. N. Lewis, *Chem. Rev.*, 1993, **93**, 2693.
- 4 A. P. Alivisatos, *Science*, 1996, **271**, 933.

- 5 G. K. Kouassi and J. Iruadayaraj, *Anal. Chem.*, 2006, **78**, 3234.
- 6 M. Brust, M. Walker, D. Bethell, D. J. Schiffrin and R. Whyman, *J. Chem. Soc., Chem. Commun.*, 1994, 801.
- 7 D. Bethell and D. Schiffrin, *J. Anal. Chem.*, 2004, **76**, 5371.
- 8 C.-H. Teng, K.-Ch. Ho, Ya-Sh. Li and Yu-Ch. Chen, *J. Anal. Chem.*, 2004, **76**, 4337.
- 9 M. A. Willard, L. K. Kurihara, E. E. Carpenter, S. Calvin and V. G. Harris, *Int. Mater. Rev.*, 2004, **49**, 125.
- 10 S. P. Gubin, Yu. A. Koksharov, G. B. Khomutov and G. Yu. Yurkov, *Usp. Khim.*, 2005, **74**, 539 (*Russ. Chem. Rev.*, 2005, **74**, 489).
- 11 Zh. Xu, Y. Hou and S. Sun, *J. Am. Chem. Soc.*, 2007, **129**, 8698.
- 12 M. Mikhaylova, D. K. Kim, N. Bobrysheva, Th. Tsakalagos and M. Muhammed, *Langmuir*, 2004, **20**, 2472.
- 13 S. Si, C. Li, X. Wang, D. Yu, Q. Peng and Y. Li, *J. Am. Chem. Soc., Cryst. Growth Des.*, 2005, **5**, 393.
- 14 A. K. Gupta and M. Gupta, *Biomaterials*, 2005, **26**, 3995.
- 15 J. L. Lyon, D. A. Fleming, M. B. Stone, P. Schiffer and M. E. Williams, *NanoLett.*, 2004, **4**, 719.
- 16 T. Hyeon, *Chem. Commun.*, 2003, 927.
- 17 P. A. Dresco, V. S. Zaitsev, R. J. Gambino and B. Chu, *Langmuir*, 1999, **15**, 1945.
- 18 W. Lingyan, P. Hye-Young, S. Lim., M. J. Schadt, D. Mott, L. Jin, X. Wang and Ch.-J. Zhong, *J. Mater. Chem.*, 2008, **18**, 2629.
- 19 B. Jie, C. Wei, L. Taotao, Z. Yulin, J. Peiyuan, W. Leyu, L. Junfeng, W. Yongge and L. Yadong, *AcsNano*, 2007, **1**, 293.
- 20 W. Lingyan, L. Jin, F. Quan, S. Masatsugu, S. Itsuko, M. H. Engelhard, L. Yuehe, K. Nam, Q. W. Jian and Ch.-J. J. Zhong, *Phys. Chem.*, 2005, **109**, 21593.
- 21 S. H. Sun, C. B. Murray, D. Weller, L. Folks and A. Moser, *Science*, 2000, **287**, 1989.
- 22 L. M. Demers, C. A. Mirkin, R. C. Mucic, R. A. Reynolds, R. L. Leitsinger and G. A. Viswanadham, *J. Anal. Chem.*, 2000, **72**, 5535.
- 23 K. L. Chung, X. Dan and M. M. F. Choi, *J. Mater. Chem.*, 2007, **17**, 2418.
- 24 D. Hobarra, S. Kondo, M.-S. Choi, Y. Ishioka, S. Hirata, M. Murata and K. Azuma, *Phys. Stat. Sol.*, 2007, **6**, 1706.
- 25 J. Lin, W. Zhou, A. Kumbhar, J. Wiemann, J. Fang, E. E. Carpenter and C. J. O'Connor, *J. Solid State Chem.*, 2001, **159**, 26.
- 26 S.-J. Cho, J.-C. Idrobo, J. Olamit, K. Liu, N. D. Browning and S. M. Kauzlarich, *Chem. Mater.*, 2005, **17**, 3181.
- 27 M. Mandal, S. Kundu, S. K. Ghost, S. Panigrahi, T. K. Sau, S. M. Yusuf and T. Pal, *J. Colloid Interface Sci.*, 2005, **286**, 187.

Received: 11th January 2010; Com. 10/3447